

21. Tori, K. U. *et al.* Functional dissection of *Arabidopsis* COP1 reveals specific roles of its three structural modules in light control of seedling development. *EMBO J.* **17**, 5577–5587 (1998).
22. McNellis, T. W. *et al.* Expression of an N terminal fragment of COP1 confers dominant-negative suppression of seedling photomorphogenic development in transgenic *Arabidopsis*. *Plant Cell* **8**, 1491–1503 (1996).
23. Joazeiro, C. A. P. *et al.* The tyrosine kinase negative regulator c-Cbl as a RING-type E2-dependent ubiquitin-protein ligase. *Science* **8**, 309–312 (1999).
24. Loric, K. L. *et al.* RING fingers mediate ubiquitin-conjugating enzyme (E2)-dependent ubiquitination. *Proc. Natl Acad. Sci. USA* **96**, 11364–11369 (1999).
25. Wei, N. & Deng, X. W. Making sense of the COP9 signalosome. *Trends Genet.* **15**, 98–103 (1999).
26. Reed, J. W. *et al.* Phytochrome A and phytochrome B have overlapping but distinct function in *Arabidopsis* development. *Plant Physiol.* **104**, 1139–1149 (1991).
27. Ahmad, M. *et al.* Cryptochrome blue-light photoreceptors of *Arabidopsis* implicated in phototropism. *Nature* **16**, 720–723 (1994).
28. Wagner, D. *et al.* Overexpression of phytochrome B induces a short hypocotyl phenotype in transgenic *Arabidopsis*. *Plant Cell*, **3**, 1275–1288 (1992).
29. Boylan, M. T. & Quail, P. H. Phytochrome A overexpression inhibits hypocotyl elongation in transgenic *Arabidopsis*. *Proc. Natl Acad. Sci. USA* **88**, 10806–10810 (1991).
30. Koegl, M. *et al.* A novel ubiquitination factor, E4 is involved in multiubiquitin chain assembly. *Cell* **96**, 635–644 (1999).

Acknowledgements

We thank R. Fry and H. Wang for reading and commenting on this manuscript, and A. Cashmore, C. Lin, P. Quail and G. Whitelam for providing *Arabidopsis* photoreceptor mutant strains. Our work was supported by grants from NIH (to X.W.D.), USDA (to N.W.) and the Human Frontiers Science Program Organization. X.W.D. is an NSF Presidential Faculty Fellow, M.T.O. is an NIH and Dept of Education predoctoral trainee and C.S.H. is a Human Frontier Science Program Organization postdoctoral fellow.

Correspondence and requests for materials should be addressed to X.W.D. (e-mail: xingwang.deng@yale.edu).

Genomic rearrangement in *NEMO* impairs NF- κ B activation and is a cause of incontinentia pigmenti

The International Incontinentia Pigmenti (IP) Consortium

* A full list of authors appears at the end of the paper

Familial incontinentia pigmenti (IP; MIM 308310) is a genodermatosis that segregates as an X-linked dominant disorder and is usually lethal prenatally in males. In affected females it causes highly variable abnormalities of the skin, hair, nails, teeth, eyes and central nervous system. The prominent skin signs occur in four classic cutaneous stages: perinatal inflammatory vesicles, verrucous patches, a distinctive pattern of hyperpigmentation and dermal scarring¹. Cells expressing the mutated X chromosome are eliminated selectively around the time of birth, so females with IP exhibit extremely skewed X-inactivation². The reasons for cell death in females and *in utero* lethality in males are unknown. The locus for IP has been linked genetically to the *factor VIII* gene in Xq28 (ref. 3). The gene for *NEMO* (NF- κ B essential modulator)/IKK γ (I κ B kinase- γ) has been mapped to a position 200 kilobases proximal to the *factor VIII* locus⁴. *NEMO* is required for the activation of the transcription factor NF- κ B and is therefore central to many immune, inflammatory and apoptotic pathways^{5–9}. Here we show that most cases of IP are due to mutations of this locus and that a new genomic rearrangement accounts for 80% of new mutations. As a consequence, NF- κ B activation is defective in IP cells.

The extreme skewing of X-inactivation observed in IP patients has implications for screening of candidate genes. Complementary DNA prepared from females with IP will not contain the mutated allele of the disease locus, so screening of candidate genes for mutation must be performed with genomic DNA. We used two

approaches to screen *NEMO*: (1) generation and sequencing of fibroblast cDNA from extremely rare cases that express only the mutated X chromosome (two male cases and one female abortus, see Methods); and (2) resolution of the *NEMO* genomic structure for mutational analysis of individual exons. Reverse transcriptase polymerase chain reaction (RT-PCR) from messenger RNA derived from skin fibroblasts from four affected fetuses (D, K, IP85m and G) and controls (C1 and C2) was conducted with *NEMO*-specific primers (Fig. 1). Male samples D and IP85m have only one X chromosome. Female sample K is unusual in that contrary X-inactivation skewing has resulted in expression of only the mutated (IP) X chromosome. Affected female G expresses both Xs, as expected for a fetal IP case that has not yet undergone selective elimination of affected cells.

Amplification between primers located in *NEMO* exons 2 and 3 (exon organization in Fig. 2) for fetuses K, D and G produced a product corresponding to the 5' end of *NEMO* cDNA. However, amplification between exons 2 and 4 produced the predicted fragment from fetus G and control RNAs but not from fetuses D and K. Thus, the 3' end of the *NEMO* cDNA is absent in fetuses K and D. This could not be explained by loss of individual exons because we could amplify all 10 coding exons from genomic DNA (not shown). These results indicate that a mutation that disturbs mRNA production may exist between primers R4 and R1 in exons 3 and 4, respectively.

In a sample from another affected male (IP85m), RT-PCR across the entire coding region of *NEMO* was successful and the products

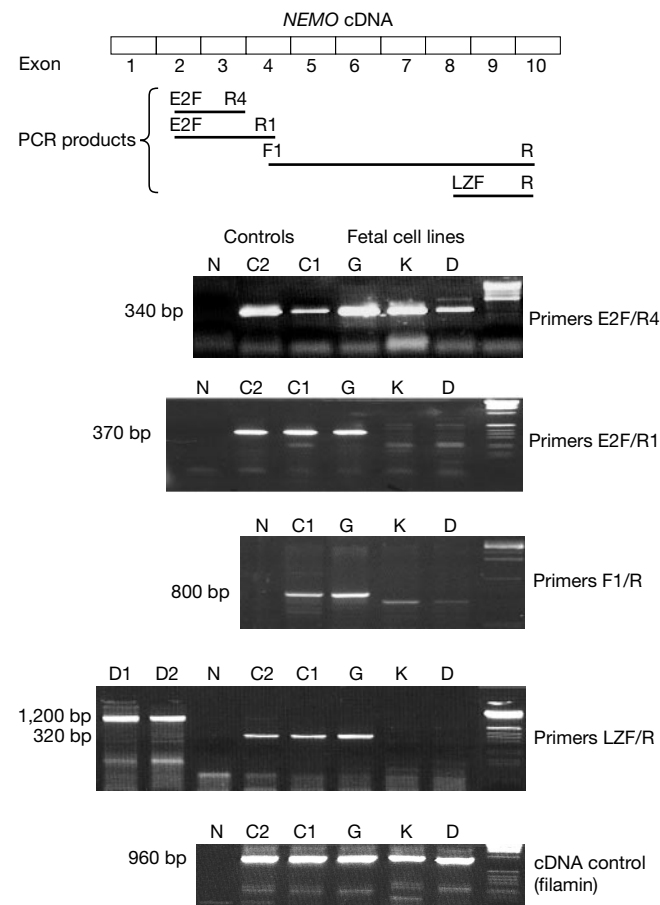


Figure 1 Amplification by RT-PCR of *NEMO* cDNA from IP patient cell lines. The positions of PCR products relative to *NEMO* exons are shown at the top. Amplification is from fetal cDNA samples G, K and D, cDNA from healthy donors (C1 and C2) and control DNA (D1 and D2). PCR of filamin cDNA from all samples acted as a control for RNA integrity. Primer sequences are given in Methods.

sequenced completely. An A-to-G change (base 1,259) was detected within the STOP codon of the mature message (see Supplementary Information). This would result in the addition of 27 residues to the carboxy terminus of the NEMO protein. Examination of the relevant region of genomic DNA (exon 10) from family IP85 revealed that the male proband's affected mother is heterozygous for the change, whereas his unaffected grandmother and grandfather have an intact STOP codon. The mutation has therefore appeared *de novo* with the disease in this family. To determine the spectrum of mutations in additional IP families, we sequenced the complete *NEMO* locus (Fig. 2). The 23-kilobase (kb) gene is composed of 10 exons with three alternative non-coding first exons^{4,5,10} (1a, 1b and 1c; Table 1). The *NEMO* gene partially overlaps the *G6PD* gene and is transcribed in the opposite direction⁴.

Exons 1–9 and the coding portion of exon 10 were amplified by PCR from 30 classically affected, unrelated IP patients (see Table 2 for primer sequences). Amplification products were screened for mutations by single-strand conformation polymorphism (SSCP), heteroduplex analysis or direct sequencing. Only four additional changes were found (Fig. 2 and see Supplementary Information). A 10-base pair (bp) insertion in exon 2 (between coding nucleotides

127 and 128) in family XL349 was found in both an IP proband and her affected mother but not in unaffected siblings. The insertion is an exact duplication of the previous 10 nucleotides, shifts the reading frame of the protein to add eight amino acids after residue 43 and then truncates the protein at the next, in-frame STOP codon. A second insertion in exon 9 of a single C (1110–1111) within a run of cytosines segregates with the disease in family XL203. This frameshift mutation would putatively append 23 new amino acids onto proline residue 370 of the translated protein. A mis-sense transition (A/G) in exon 10 that changes a methionine to a valine in the C terminus of the NEMO protein (M407V) was found in an affected female from family 72. SSCP analysis showed that this relatively conservative change segregates with the disease through a three-generation pedigree. Finally, a C-to-T (C184T), proline to STOP codon mutation found in exon 2 in family XL352 predicts a truncated protein consisting of the amino-terminal 61 amino acids of NEMO. These mutations were not detected in more than 60 unrelated X chromosomes. In addition to apparently pathogenic changes, a polymorphism in exon 1c in the 5' untranslated region (–165 from exon1c and 5,678 of the *NEMO* genomic sequence) changes a C to a G in 6 out of 40 chromosomes.

Surprisingly few mutations were detected by screening individual

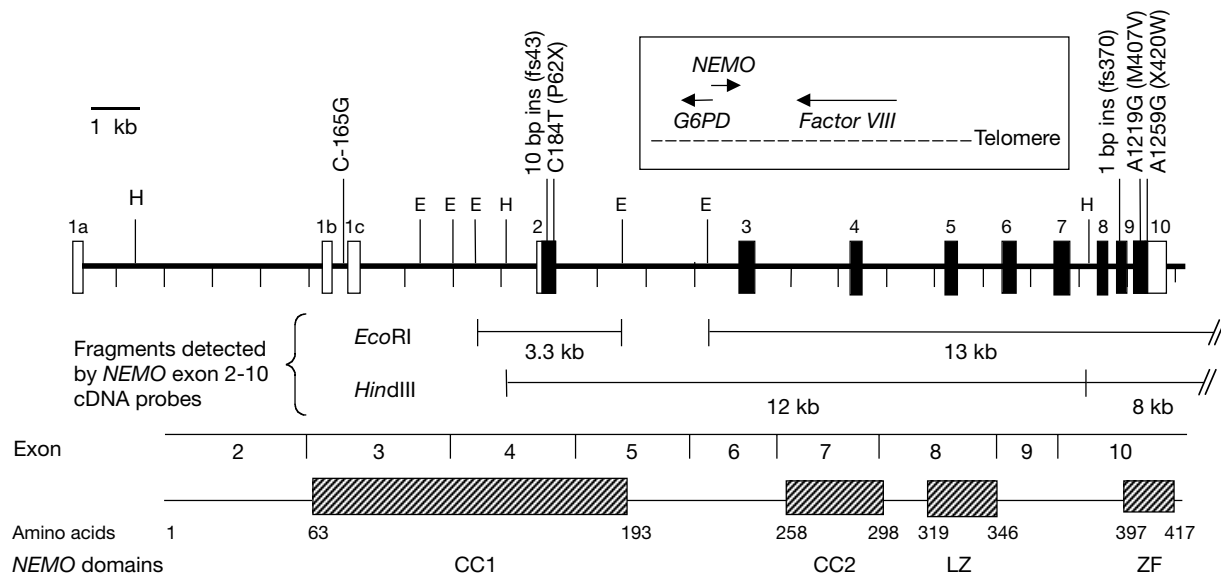


Figure 2 Genomic structure of the *NEMO* gene and partial restriction map (H, *Hind*III; E, *Eco*RI). The 10 exons span 23 kb of genomic sequence. Non-coding (open boxes) and coding exons (filled boxes) are shown. Three alternative first exons numbered 1a, 1b and 1c are found spliced to exon 2. The positions of intragenic mutations, a common polymorphism and restriction fragments seen on Southern blots are shown. The

relationship of coding exons 2–10 to the two coiled-coil (CC1 and CC2), leucine zipper (LZ) and zinc finger (ZF) motifs of the NEMO secondary structure is illustrated. Inset, the orientation of *NEMO* to *factor VIII*, *G6PD* and the Xq28 telomere (not to scale) with arrows in a 5' → 3' direction.

Table 1 Intron-exon structure of the human *NEMO* gene

Intron	Size (bp)	Donor*	Acceptor*
1a	5,263	GTCCCATCAGgtgggaaaag	gaagggcgacCGCGAAACTG
1b	174	CTGCTGACAGgtgtggctct	acttggggcggCGAGCTGGAC
1c	3,889	TGGCAGCTAGgtatctgatt	tctcttccagCCCTTGCCCT
2	3,981	GAGCTCCGAGgtgaggaaaag	ctgccaccagATGCCATCCG
3	2,155	ATGCCAGCAGgtagtccggg	tatctctgcagCAGATGGCTG
4	1,757	TGGAGGTTCgtgagtcggg	ccggtgccagGGCCCGGCG
5	1,128	CGGAGGAGAgtgagtcagc	ctttcctcagGAGGAAGCTG
6	1,023	CGGGAAGCGagtgagtcgga	cgctcttagGGAATGCAGC
7	607	GAAGGCCAGgtgagggccc	gatttgccagCGGCATATCT
8	257	AGTCGGCCAGgtgggcctct	gttttcaagGATCGAGGAC
9	298	CCGCCCTGgtgagtgagc	ctttcccgCCTACCTCTC

* Upper case denotes exon sequence, lower case denotes intron sequence.

exons of *NEMO* in IP patients. Moreover, amplification and sequencing of all coding exons failed to detect any mutation in fetuses K and D that could explain the abnormal mRNA structure. We therefore investigated the possibility of genomic rearrangement by Southern blotting. Genomic DNAs from IP patients and healthy individuals were digested with *HindIII* and *EcoRI* and hybridized to a probe representing the coding region of *NEMO* cDNA. In addition to the expected wild-type fragments (12-kb and 8-kb *HindIII*, 13-kb and 3.3-kb *EcoRI*), we found a novel 8-kb *HindIII* band and a novel 2.8-kb *EcoRI* band for 38 out of 47 unrelated IP patient samples (Fig. 3a). The novel fragments were concordant for the two enzymes in all cases and were absent for the affected male (IP85m, above) containing a mutation in the termination codon (not shown). The novel bands segregated with disease in each pedigree analysed. In two families an *EcoRI* band of about 14 kb was observed along with the novel 2.8-kb band (for example, IP64, Fig. 3a), with a concomitant reduction in signal for the wild-type 13-kb band. This band did not segregate with disease in these families and is therefore a non-pathogenic variant.

The appearance of novel bands is associated with the development of IP. For two families with sporadic cases (IP44 and IP91) the novel bands (8-kb *HindIII* and 2.8-kb *EcoRI*) were found in the proband's DNAs but not the parents' and have therefore appeared *de novo* with the disease (Fig. 3b). To determine whether the new bands resulted from a deletion, we screened hemizygous DNA from a male abortus whose mother carries the rearrangement (IP1m). This male is from a four-generation IP family (IP1; ref. 11) and has inherited the IP haplotype from his affected mother (data not shown). *NEMO* exons 1a–10 could be amplified by PCR. When DNA from this male was analysed by Southern blotting, 13-kb and 3.3-kb wild-type *EcoRI* bands and the novel 2.8-kb band were seen (lane 12, Fig. 3b). As only one X chromosome is present in this fetus, more than one sequence homologous to the *NEMO* gene must be assumed. The presence of a doublet of hybridizing *HindIII* fragments at about 12 kb in all lanes implies that at least part of *NEMO* is also duplicated in wild-type DNA. Complementary DNA probes encompassing coding sequences from exons 2 and 3 detected the novel IP-specific fragments but probes containing sequences from exons 4–10 did not. Furthermore, hybridization with single exons revealed that exon 3, but not exon 2 or 4, is present on the novel *EcoRI* fragment, whereas exons 2 and 3 but not 4 hybridize to the novel *HindIII* band (not shown).

To investigate whether intronic sequences are involved in the rearrangement, DNA from the male abortus (IP1m) was used to amplify across *NEMO* introns. Amplification across single introns (with forward and reverse primers flanking individual exons; Table 2) was successful for all introns (not shown). However, differences were found compared with controls when PCR reactions were anchored at exon 2 (Fig. 3c). In the affected male (IP1m), amplification could proceed from exon 2 to exon 3 but not from exon 2 to exons 4, 5, 6 or 7. The mutation therefore involves disruption within intron 3. Anchoring the PCR reactions at exons 3 or 7, however, yielded wild-type products for all combinations with downstream exons (Fig. 3c). This is compatible with the existence of a putative second copy of *NEMO* that contains exons 3–10 but not exons 1 and 2. This second copy must be highly homologous: sequencing of long-range PCR products from IP1m revealed that copies of exon 3 in tandem with either exon 2 or exon 4 were identical. Importantly, analysis of DNA from IP-affected male fetus D yielded results similar to those obtained for IP1m for both long-range PCR and Southern blotting, indicating that the common genomic rearrangement is responsible for the production of aberrant *NEMO* mRNA lacking sequences from exons 4–10 as described above. Our RT-PCR, Southern and genomic PCR data indicate that a common rearrangement within intron 3 of *NEMO* generates novel restriction fragments that contain exon 3.

We used this information to isolate the boundary of rearrangement neighbouring exon 3 within the 2.8-kb novel *EcoRI* band. DNA from the male abortus (IP1m) was digested with *EcoRI* and ligated to pre-annealed adapter oligonucleotides with *EcoRI* cohesive ends (see Methods). Nested PCR between adapter primers and exon-3-specific forward primers yielded a product of about 2 kb that was sequenced completely. The fragment was found to extend from exon 3 into intron 3 for 1.8 kb. The sequence then diverged from intron 3 identity after a position equivalent to 15,749 of the *NEMO* genomic sequence; a novel 104-bp sequence was found between this boundary and the *EcoRI* site. Interestingly, the boundary between intron 3 and this sequence coincides precisely with the end of a repeat of the MER67B family in intron 3. The 104-bp sequence, which itself is homologous to an L2 repeat, was used to screen available sequence data from Xq28 BAC clones and found within a short sequence contig from BAC clone 211L10, which also contains the *NEMO* gene (for sequence see Supplementary Information).

Table 2 Primers and conditions for PCR amplification of individual exons

Exon	Length (bp) Product size (bp)	Forward primer (5' → 3')	Reverse primer (5' → 3')
1a	125 302	GGA AGT CAG CCC AGA AAT GT	GTA CTT ACT GCC CCC TTC CA
1b	95 297	GGG CGG GGC TTG TGT TTT TA	AGA AGC GCG GAG CAG GAA CG
1c	170 334	TTC CTG CTC CGC GCT TCT GG	CCA GGA GAG CCC ATT CAT TC
2	202 321	TCT GCT GGG TAA GGA TGT GG	TCT GCA GGT GGG GAG AAG AC
3	212 296	CCC AGC TCC CCT CCA CTG TC	CAC CTG GCG TCA CTC GGC GGG T
4	119 194	CAG TGC TGA CAG GAA GTG GC	AAC CCT GGA AGG GGT CTC CGG AG
5	153 351	CAT CAG CTC GCA GTC ACA GG	CCG ACA CTT CTC AGC CTT TC
6	97 277	AAG GGG GTA GAG TTG GAA GC	AGG CAA GTC TAA GGC AGG TC
7	144 347	GCC ACT CTT TCA TCC TTC TC	CTG GGC AAC AAG AGC AAA AC
8	143 245	TGC CTG GTG GGT GGC TGG CT	CAG TGT GCG ACC CAC TGC TCA
9	62 234	GCT GCT TTG ACA CTA GTC CA	CAG AGA GCA ACA GGA AGG TC
10	728 363	CGG CGG CTC CTG GTC TTA CA	GCC ACC CAG CCC TTC ATC CT

To confirm that the novel sequence is associated with the rearranged 2.8-kb *EcoRI* fragment, we conducted PCR between exon 3 and the novel boundary sequence for families with and without the common rearrangement found on Southern blots (Fig. 3d). The resulting 2-kb band occurs only in IP patients who have been shown to carry the altered band by Southern blotting, not in controls and parents of sporadic cases, and is a simple diagnostic PCR test for 80% of IP cases. The presence of a 13-kb band in patients or controls without the rearrangement suggested that the natural site for the boundary sequence may be 3' of *NEMO*. End sequencing of both this band and a 13-kb *EcoRI* fragment housing exons 3–10 of *NEMO* from BAC clone 211L10 confirmed this hypothesis. Furthermore, at this downstream location sequences identical to the MER67B of intron 3 were found juxtaposed to the 104 bp of L2 repeat in the same orientation as in the *NEMO* gene. Further PCR and sequencing indicated that although 870 bp of intron 3 is repeated 3' of the *NEMO* gene, there is no additional exon 3 within this fragment.

The most common mutation in IP is therefore a deletion of part of the *NEMO* gene mediated by directly repeated sequences within intron 3 and 3' of exon 10 (Fig. 3e). The translocation of sequences

from this downstream region to intron 3 can explain the novel band sizes observed on Southern blots, as *EcoRI* and *HindIII* sites are found at appropriate 3' positions. That the rearrangement gives rise to aberrant *NEMO* message has also been proved by RT-PCR amplification between L2 primer JF3R and exon 3 forward primers on cDNA from fetus D and K (not shown). This revealed that at least 26 novel amino acids would be appended to the 133 residues of *NEMO* encoded by exons 2 and 3. A second, homologous but incomplete copy of the *NEMO* gene, suggested by Southern and PCR data, appears to be unaltered by the IP mutation (Fig. 3e). IP therefore joins a growing list of disorders caused most frequently by genomic rearrangement¹². The origin of the genomic rearrangements often shows a predilection for one parent. For example, homologous recombination between tandem repeats leading to *de novo* duplication in CMT1A occurs primarily during male gametogenesis¹³. For IP, two-thirds of new mutations originate from fathers, consistent with paternal bias for rearrangement². The origin of mutation has been established for 12 patients with the rearrangement. Ten occurred during male gametogenesis, implicating intrachromosomal interchange. In cases of genomic rearrangement, it is important to ascertain whether more than one

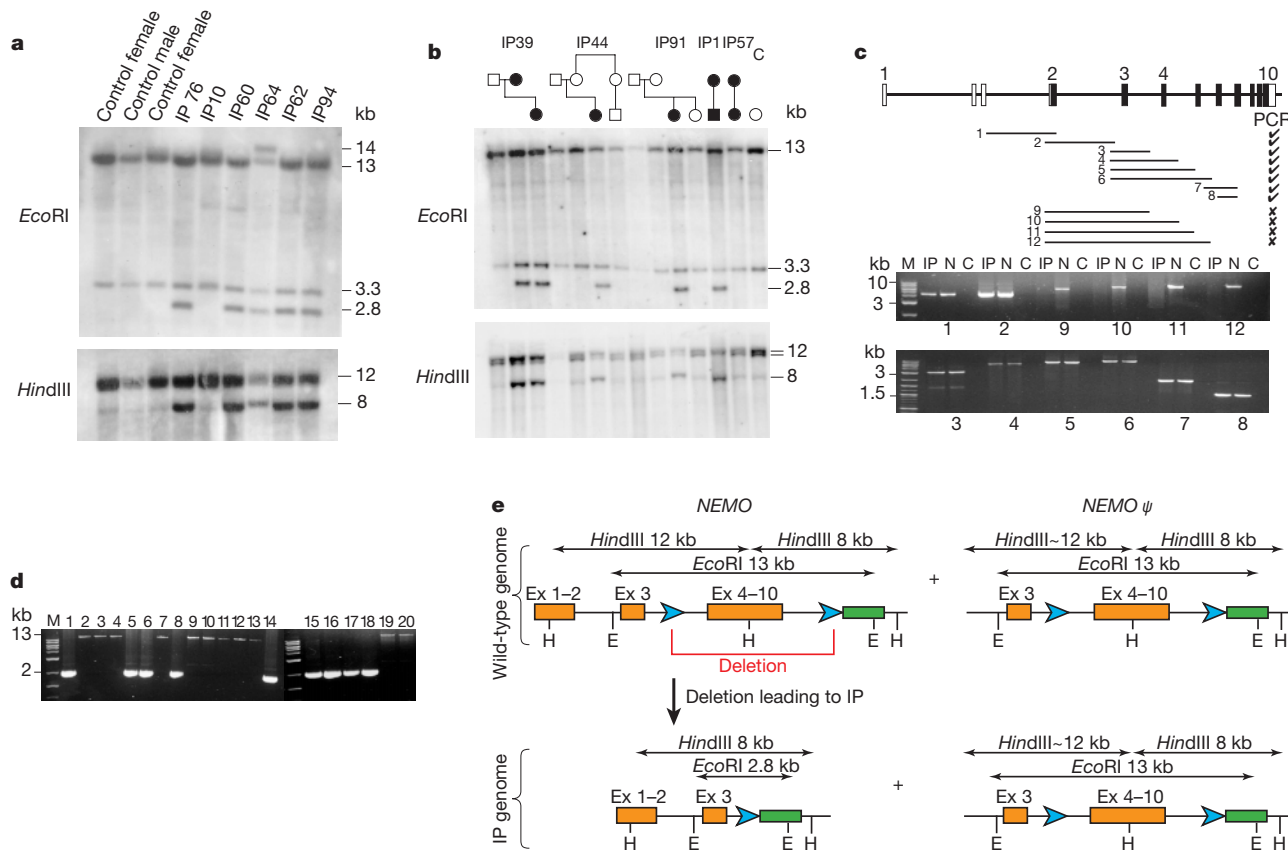


Figure 3 Genomic rearrangement in IP patients. **a**, Southern blot hybridized with *NEMO* cDNA representing exons 2–10 showing the appearance of new *EcoRI* (2.8 kb) and *HindIII* (8 kb) bands in unrelated IP females compared with controls. IP10 does not show these bands for either enzyme. A female in family IP64 also has a novel 14-kb band that does not segregate with disease. For *HindIII*, a doublet of bands at 12 kb is seen instead of the expected single band in addition to bands corresponding to exons 7–10 (faint 8-kb band). **b**, Novel *EcoRI* and *HindIII* bands appear *de novo* with the disease in sporadic cases of IP (IP44 and IP91). Segregation in family 39 is also shown. A male sample from family IP1 carrying the rearrangement still retains wild-type *EcoRI* bands although the smaller of the doublet *HindIII* bands has disappeared. **c**, Long-range PCR across the *NEMO* gene in male patient IP1m. Schematic shows 12 PCR reactions conducted in patient (IP) versus control (N) samples, and the gel shows the products. Ticks, successful

amplification in IP1m; crosses, lack of amplification. **d**, Diagnostic PCR in IP patients with the rearrangement. Amplification between exon 3 forward primer 3FH and a primer from the L2 repeat in the rearranged *EcoRI* fragment (JF3R) gives a 2-kb band only in IP samples (lanes 1, 5, 6, 8, 14–18). A 13-kb band is seen in control samples that do not have the rearrangement (lanes 2–4, 7, 9–13, 19, 20). **e**, Model for IP rearrangements. In addition to the *NEMO* gene (left), a *NEMO* pseudogene lacking exons 1 and 2 is proposed (right, *NEMO*ψ). An 870-bp region of identity corresponding to a MER67B repeat (arrow) exists both in intron 3 and 3' to exon 10. An L2 repeat follows the 3' MER67B sequence at the downstream site (hatched box). Recombination between the regions of identity will delete exons 4–10 of *NEMO*. Diagnostic PCR between exon 3 and the L2 sequence yields a 2-kb band in patients and a 13-kb band in controls.

gene is involved. Of the nine out of 47 IP patients found not to have a rearrangement, six have been screened for intragenic changes and four found to have mutations (above). These segregate with the disease in families or have arisen *de novo* with the disease, indicating that defects in *NEMO* alone are sufficient to cause the disorder.

NEMO is essential in the NF- κ B activation process⁹. NF- κ B homo- or heterodimers are sequestered in the cytoplasm through interaction with an inhibitory molecule of the I κ B family. Upon cytokine stimulation, the I κ B molecules are phosphorylated, poly-ubiquitinated and degraded through the ubiquitin–proteasome pathway^{6,14}. NF- κ B is then free to translocate to the nucleus and to activate its target genes. This phosphorylation event is carried out by a high molecular mass, multiprotein kinase complex containing two subunits with kinase activity (IKK1/ α and IKK2/ β). The third known component of this IKK complex is NEMO (IKK γ , IKKAP or IKBKG Human Gene Nomenclature)^{5,7,9}, a protein with relative molecular mass 48,000 (M_r 48K). NEMO has no apparent catalytic activity; it interacts directly with the kinase subunits and is required for activation of the kinase complex in response to extracellular (or intracellular) stimuli. Its absence results in a complete inhibition of NF- κ B activation. We therefore determined whether NF- κ B activation was defective in IP patients K and D, who express only mutated

NEMO, compared with controls. These patients possess the common rearrangement found in 80% of IP cases.

We analysed cytoplasmic extracts from primary embryonic fibroblasts by western blotting for the abundance of the three known subunits of IKK (IKK-1, IKK-2 and NEMO), the two major subunits of NF- κ B (p50 and relA) and two I κ B species (I κ B α and β) (Fig. 4a). No 48K band corresponding to the NEMO molecule was detected in fibroblasts from patients K and D compared to controls, although a low relative molecular mass band of about 21K was seen. This may represent the truncated version of NEMO predicted from genomic and RT–PCR analysis. Analysis of IKK-1, IKK-2, p50 and relA protein levels did not reveal any significant differences between patients and controls. However, a substantial increase in I κ B α and I κ B β was seen in fibroblasts from patients K and D. As the stability and levels of I κ Bs are controlled by NF- κ B, this observation indicated that the NF- κ B system may be perturbed in IP patients.

NF- κ B activation was measured in embryonic fibroblasts from patients K and D with an electrophoretic mobility shift assay (Fig. 4b). Upon stimulation with tumour necrosis factor (TNF), two retarded complexes were observed with nuclear extracts prepared from normal and patient G embryonic fibroblasts. A supershift experiment showed that the upper complex was composed of both

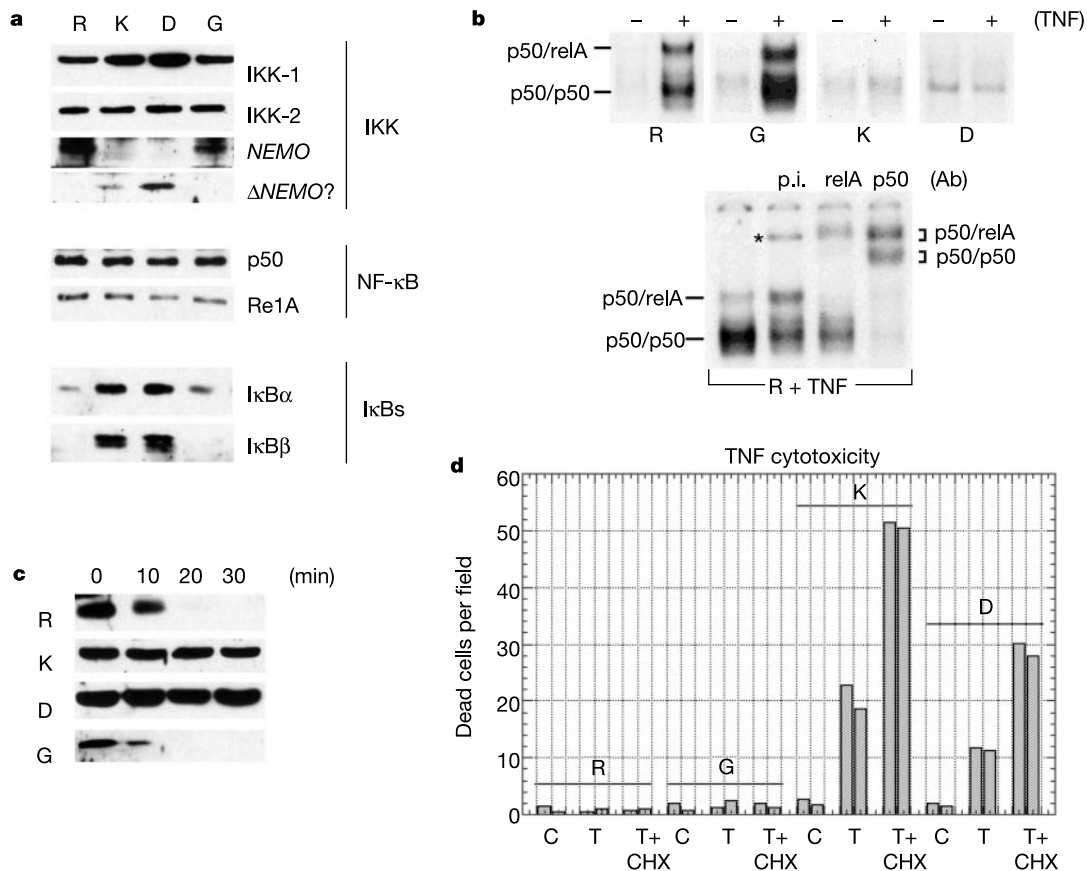


Figure 4 Defective NF- κ B activation in IP cells. **a**, NEMO is not detected in IP embryonic fibroblasts. Cytoplasmic extracts derived from normal, G, K or D embryonic fibroblasts were subject to western blotting with antibodies directed against NEMO, IKK-1, IKK-2, p50, relA, I κ B α and I κ B β . Δ NEMO, putative truncated version of NEMO found only in patients K and D. **b**, NF- κ B is not activated in IP embryonic fibroblasts. Top, normal fibroblasts or those derived from patients G, K or D were mock- or TNF α -treated. Retarded complexes corresponding to p50/relA and p50/p50 dimers (see below) are indicated. Bottom, nuclear extracts prepared from TNF-treated normal embryonic fibroblasts were pre-incubated with pre-immune serum (p.i.) or with anti-relA or p50 sera, then analysed

with an EMSA. Asterisk, nonspecific band generated with the p.i. serum. Supershifted p50/relA and p50/p50 dimers are indicated. **c**, I κ B α degradation is defective in IP embryonic fibroblasts. Normal cells or those derived from patients G, K or D were treated with TNF α (10 ng ml⁻¹) for the indicated times, and cytoplasmic extracts were prepared and analysed, after western blotting, with anti-I κ B α antibody. **d**, IP embryonic fibroblasts are TNF-sensitive. Normal cells or those derived from patients G, K or D were mock (C), TNF α (T) or TNF α plus cycloheximide (T+CHX)-treated for 20 h, and the cell viability was determined through trypan blue exclusion. One experiment, out of two giving similar results, is shown.

p50 and relA proteins, whereas the lower one was composed of p50 only (Fig. 4b). Importantly, neither p50/relA nor p50/p50 complex was induced in nuclear extracts derived from TNF-treated embryonic fibroblasts from patients K and D, indicating a complete defect in the NF- κ B activation process. A similar observation was made when interleukin-1 (IL-1) was used instead of TNF (data not shown).

As the translocation of NF- κ B to the nucleus results from degradation of I κ B, the fate of I κ B α in normal and IP embryonic fibroblasts after treatment with TNF or IL-1 was determined. Whereas patient G and control fibroblasts exhibited complete disappearance of I κ B α after 40 min of TNF or IL-1 treatment, no such disappearance could be observed in cells from patients K and D (Fig. 4c, and data not shown).

In several cell types, including embryonic fibroblasts, NF- κ B protects against TNF-induced apoptosis¹⁵. We investigated the sensitivity of normal and IP embryonic fibroblasts to TNF (Fig. 4d). In contrast to cells from controls or patient G, which were unaffected by treatment with TNF or TNF and cycloheximide, embryonic fibroblasts from patients K and D were sensitive to TNF and this sensitivity was increased by cycloheximide. These data demonstrate a lack of NF- κ B activation in IP embryonic fibroblasts, resulting from a defect at the level of the NEMO molecule. As a consequence, IP cells are highly sensitive to pro-apoptotic signals.

Can the pathology observed in male and female IP patients be explained in terms of NEMO function? The genes encoding components of the IKK complex have been inactivated by homologous recombination in the mouse. Inactivation of IKK2 resulted in embryonic death due to massive liver apoptosis at day 14 (for a review see ref. 6), whereas that of NEMO resulted in death of male embryos at day 12 with a similar phenotype¹⁶ (murine NEMO is also X-linked). A similarly marked phenotype was observed when the gene encoding relA, the most potent transcriptional activator of the NF- κ B family, was inactivated¹⁷. This phenotype was due to the pro-apoptotic effect of TNF¹⁸, in keeping with the high sensitivity to TNF-induced apoptosis observed in cell lines derived from IP patients. In both mice and humans, therefore, the complete absence, or strong reduction, of NF- κ B activity results in embryonic lethality.

A prominent role for NF- κ B in the apoptotic response also has a bearing on the phenotype in heterozygous females. It is likely that skewing of X-inactivation, at least in blood, results from progressive apoptotic elimination of cells bearing mutated *NEMO* on the active X chromosome. For *NEMO*-deficient heterozygous female mice, a phenotype comparable to that seen in man has not yet been reported. Owing to lyonization, however, understanding the effects observed in human patients is difficult. Further clues emerge from targeting of other components of the NF- κ B pathway in mouse¹⁹. The individual inactivation of four of the five known members of the NF- κ B family results in more or less severe defects in the immune response. More interestingly, mice devoid of both the p105/p50 and the p100/p52 subunits fail to generate mature osteoclasts, causing severe osteopetrosis^{20,21}. Osteoclasts are also essential for tooth eruption as they resorb the alveolar bone to form an eruption pathway, and eruption abnormalities are a prominent feature of the human IP phenotype. Mice carrying inactivation of IKK1 (refs 22–24) exhibit almost intact activation of NF- κ B by pro-inflammatory stimuli, but show defects in morphogenetic events, including limb and skeletal patterning, and proliferation and differentiation of epidermal keratinocytes. At the skin level, NF- κ B appears to have a dual role: it controls cell growth in the stratified epithelium and regulates apoptosis. Defects in both pathways may explain the characteristic skin lesions observed in IP. Also reminiscent of the abnormalities observed in female IP patients are the deformed incisors and lack of hair follicles in the IKK1^{-/-} mice.

The phenotype observed in a surviving male with a mutation in *NEMO* (IP85m) provides a unique view of the consequences of impaired NF- κ B function in man. Severely compromised immune

cell function, lack of teeth and osteopetrosis (see Methods) are consistent with mouse models of defective NF- κ B function. A comparison can be made between the phenotype in IP85m and that of patients with familial expansile osteolysis (FEO, or familial Paget disease of bone, PDB). This is an autosomal dominant disorder characterized by focal areas of increased bone remodelling. In contrast to our findings, activating mutations in the gene for a positive activator of NF- κ B function (RANK) have been found to account for this disorder in two families²⁵. Interestingly, IP85m also showed signs of capillary bed abnormalities, both in the skin and the gut, suggesting an unsuspected role for NF- κ B in the maintenance of blood vessel architecture.

The chromosomal rearrangement found in most patients would result in a truncated molecule carrying the 133 N-terminal amino acids of NEMO plus an unknown number of novel residues. This molecule would contain part of the first coiled-coil domain (Fig. 2), and may still interact with IKK-2 but is unlikely to respond to upstream signals. The mutation in family XL349 results in a NEMO molecule consisting of only 61 N-terminal amino acids. This short peptide could not interact with IKKs and is probably inactive. The insertion that introduces a frameshift after amino acid 370 results in the replacement of the entire C-terminal, zinc finger domain with 23 unrelated amino acids. Deletion of this zinc finger domain results in a severe loss of function of the NEMO molecule in complementation assays (G.C. and A.I., unpublished data). Thus, with rare exceptions, mutations causing IP severely truncate the NEMO protein and result in loss of function.

An interesting mutation is that affecting the STOP codon in male patient IP85m. A likely explanation for this milder phenotype is partial loss of NEMO function, raising the possibility that mis-sense mutations with only minor effects on NEMO function may cause a less morbid phenotype. Therefore, mis-sense mutations in *NEMO* may contribute to a wide range of conditions related to IP such as immune deficiency, osteopetrosis, and dental and ophthalmological abnormalities. □

Methods

Collection of families and preparation of samples

Families with IP were ascertained with ethical committee approval at the collaborating institutions. All affected females had a history of perinatal blistering and at least one other stage of skin lesions, dental, and/or eye, and/or central nervous system abnormalities.

Fibroblast lines

Primary fibroblast cultures expressing a mutant IP X chromosome were available from four subjects. Fetus K was a spontaneously aborted, affected female belonging to a three-generation IP family. Lethality in this case was associated with exclusive expression of the maternal X chromosome bearing the IP mutation, presumably because a deleterious mutation is present on the opposing X or for stochastic reasons. (A.S. *et al.*; manuscript in preparation). Fetus D was a spontaneously aborted, affected male with an affected mother. Fetus G was a medically interrupted affected female belonging to a large IP family. X-inactivation was random in this line. IP85m was the affected son of a classically affected IP female. He was born with multiple capillary hemangiomas, developed lymphodema of the lower limbs and failed to thrive owing to malabsorption. Despite a destructive red blood cell picture and recurrent infections due to poor immune cell function, he survived two and a half years then succumbed to a tuberculosis infection. He had operations to remove his spleen and a gut stricture, and biopsies revealed abnormal capillary beds in the gut, extrahepatic erythropoiesis and osteopetrosis. His skin developed a reticular pigmentation. His cognitive development was normal.

DNA technology and mutation screening

DNA was extracted from fibroblasts or lymphoblasts. Southern blots were conducted with neutral transfer onto Immobilon NY+(Millipore) and ultraviolet crosslinking. PCR amplification of individual NEMO exons was conducted with Amplitaq gold and primers described in Table 2. Long-range PCR was conducted using EXPAND long template PCR system (Roche Molecular Biochemicals). DNA sequencing was conducted with BigDye terminator cycle sequencing (Perkin Elmer). SSCP and Heteroduplex analyses were done as described^{26,27}.

RNA isolation and RT-PCR

Poly A+ RNA was isolated from fibroblast cultures with Ingenious Mini Message Maker (R&D Systems) and cDNA prepared with the AmpGold RNA PCR system (Perkin Elmer) and random primers. Primers used for amplification of NEMO cDNA:

E2F(CCCTTGGCCCTGTTGGATGAAT), R(CGTCCTCGGCAGGCAGTGGCC), F1(GGCCACTGCGCTGCCGAGGACG), R1(ACCCCTCCAGAGCTGGCATTG), R4(CTTCAGATCGAGCTTCTCGAG), LZ(F(GCGGACTCCAGGCTGAGAGG).

Genomic sequencing of the NEMO gene

The NEMO gene was contained within BAC clone 211L10 from RPC111 (human male BAC library) (S.A. *et al.*, manuscript in preparation). The gene sequence was determined by a combined strategy of shotgun sequencing of M13 subclones and long-range genomic PCR products. BAC DNA was sonicated and the ends repaired with T4 DNA polymerase. Fragments of 1–2 kb were fractionated from the mixture by agarose gel electrophoresis and subcloned into M13mp18 vector prepared by digestion with *Sma*I. We screened 20,000 clones and sequenced 120 NEMO-positive M13 clones. Sequence traces were assembled with Applied Biosystem's FACTURA and INHERIT programs. Gaps were then closed with PCR to amplify the intervening material. The exon–intron boundaries are given in Table 1. The gene is listed under accession number AJ271718.

Adapter PCR of the intron 3 rearrangement boundary

DNA from a male abortus with the NEMO rearrangement from family IP1 (ref. 11) was digested with *Eco*RI and purified by ethanol precipitation. We pre-annealed 750 pmol of adapter primers Eco adapt1 (CTAATCAGACTCACTATAGGGCTCGAGCAGCCTCCGAGGGCAG) and Eco adapt2 (P-AATTCTGCCCTCGGAG) by denaturing in 30 µl buffer (5 mM Tris pH 7.4, 50 mM MgCl₂). Genomic DNA (100 ng) was ligated to a 250-fold molar excess of pre-annealed adapter primers in a 10 µl ligation reaction with T4 DNA ligase and manufacturers buffer (NEB). Primers AP1 (CCATCCTAATACGACTCACTA-TAGGGC) and intron2/exon 3 forward primer 3F (CCCAGCTCCCCTCCACTGTGTC) were incorporated into a primary PCR reaction with the EXPAND long template PCR system (Roche Molecular Biochemicals). A nested reaction with adapter primer AP2 (TCAC-TATAGGGCTCGAGCAGC) combined with a primer F3 from within exon 3 (CGGCA-GAGCAACCAGATTCTGC) yielded a 2-kb fragment. Diagnostic PCR across the boundary in IP patients was performed with 3FH (GACCAGTCCCCTCCACTGTGTC) forward primer, JF3R (CTCGGAGACAGAACCCAGCA) reverse primer and system 2 of the EXPAND kit (annealing temperature 65 °C, 10 cycles of 7-min extension and 20 cycles with increments of 20 s per cycle).

NF-κB function in IP fibroblast lines

Recombinant human interleukin-1α was from Biogen. Recombinant human TNFα was from PreproTech. Cycloheximide was from Sigma. Antisera: anti-NEMO⁹ anti-p50 1141 and anti-relA 1226 (ref. 28), anti-IκBβ 30715 (ref. 29). Purified polyclonal antibody directed against IKK-2 and IκBα were from Santa Cruz. IKK-1 monoclonal antibody was from Pharmingen. Preparation of cell extracts, western blot analysis and electrophoretic mobility shift assays were performed as described³⁰. For cytotoxicity assays, cells were treated for 20 h in complete growth medium with 20 ng ml⁻¹ TNFα or 20 ng ml⁻¹ TNFα plus 300 ng ml⁻¹ cycloheximide. Viability of cells was estimated by trypan blue exclusion.

- Landy, S. J. & Donnai, D. Incontinentia pigmenti (Bloch–Sulzberger syndrome). *J. Med. Genet.* **30**, 53–59 (1993).
- Parrish, J. E., Scheuerle, A. E., Lewis, R. A., Levy, M. L. & Nelson, D. L. Selection against mutant alleles in blood leukocytes is a consistent feature in Incontinentia Pigmenti type 2. *Hum. Mol. Genet.* **5**, 1777–1783 (1996).
- Smahi, A. *et al.* The gene for the familial form of incontinentia pigmenti (IP2) maps to the distal part of Xq28. *Hum. Mol. Genet.* **3**, 273–278 (1994).
- Jin, D. Y. & Jeang, K. T. Isolation of full-length cDNA and chromosomal localization of human NF-kappaB modulator NEMO to Xq28. *J. Biomed. Sci.* **6**, 115–120 (1999).
- Rothwarf, D. M., Zandi, E., Natoli, G. & Karin, M. IKK-γ is an essential regulatory subunit of the IκB kinase complex. *Nature* **395**, 297–300 (1998).
- Rothwarf, D. & Karin, M. The NF-κB activation pathway: a paradigm in information transfer from membrane to nucleus. *Science's Signal Transduction Knowledge Environment* (cited 26 October 1999) (http://www.stke.org/cgi/content/full/OC_sigtrans:1999/5/re1) (1999).
- Mercurio, F. *et al.* IκB kinase (IKK)-associated protein 1, a common component of the heterogeneous IKK complex. *Mol. Cell. Biol.* **19**, 1526–1538 (1999).
- Israël, A. The IKK complex: an integrator of all signals that activate NF-κB? *Trends Cell Biol.* **10**, 129–133 (2000).
- Yamaoka, S. *et al.* Complementation cloning of NEMO, a component of the IκB kinase complex essential for NF-kappaB activation. *Cell* **93**, 1231–1240 (1998).
- Li, Y. *et al.* Identification of a cell protein (FIP-3) as a modulator of NF-kappaB activity and as a target of an adenovirus inhibitor of tumor necrosis factor alpha-induced apoptosis. *Proc. Natl Acad. Sci. USA* **96**, 1042–1047 (1999).
- Jouet, M. *et al.* Linkage analysis in 16 families with incontinentia pigmenti. *Eur. J. Hum. Genet.* **5**, 168–170 (1997).
- Lupski, J. R. Genomic disorders: structural features of the genome can lead to DNA rearrangements and human disease traits. *Trends Genet.* **14**, 417–422 (1998).
- Lopes, J. *et al.* Sex-dependent rearrangements resulting in CMT1A and HNPP. *Nature Genet.* **17**, 136–137 (1997).
- Ghosh, S., May, M. J. & Kopp, E. B. NF-κB and rel proteins: Evolutionary conserved mediators of immune responses. *Annu. Rev. Immunol.* **16**, 225–260 (1998).
- Van Antwerp, D. J., Martin, S. J., Kafri, T., Green, D. R. & Verma, I. M. Suppression of TNF-α-induced apoptosis by NF-κB. *Science* **274**, 787–789 (1996).
- Rudolph, D. *et al.* Severe liver degeneration and lack of NF-κB activation in NEMO/IKKγ-deficient mice. *Genes Dev.* **14**, 854–862 (2000).
- Beg, A. A., Sha, W. C., Bronson, R. T., Ghosh, S. & Baltimore, D. Embryonic lethality and liver degeneration in mice lacking the RelA component of NF-κB. *Nature* **376**, 167–170 (1995).

- Doi, T. S. *et al.* Absence of tumor necrosis factor rescues RelA-deficient mice from embryonic lethality. *Proc. Natl Acad. Sci. USA* **96**, 2994–2999 (1999).
- Attar, R. M. *et al.* Genetic approaches to study rel/NF-κB/κB function in mice. *Semin. Cancer Biol.* **8**, 93–101 (1997).
- Franzoso, G. *et al.* Requirement for NF-κB in osteoclast and B-cell development. *Genes Dev.* **11**, 3482–3496 (1997).
- Iotsova, V. *et al.* Osteopetrosis in mice lacking nf-kappa-b1 and nf-kappa-b2. *Nature Med.* **3**, 1285–1289 (1997).
- Hu, Y. L. *et al.* Abnormal morphogenesis but intact IKK activation in mice lacking the IKKα subunit of IκB kinase. *Science* **284**, 316–320 (1999).
- Li, Q. T. *et al.* IKK1-deficient mice exhibit abnormal development of skin and skeleton. *Genes Dev.* **13**, 1322–1328 (1999).
- Takeda, K. *et al.* Limb and skin abnormalities in mice lacking IKKα. *Science* **284**, 313–316 (1999).
- Hughes, A. E. *et al.* Mutations in TNFRSF11A, affecting the signal peptide of RANK, cause familial expansile osteolysis. *Nature Genet.* **24**, 45–48 (2000).
- Alonso, A., Martin, P., Albarran, C., Garcia, O. & Sancho, M. Rapid detection of sequence polymorphisms in the human mitochondrial DNA control region by polymerase chain reaction and single-strand conformation analysis in mutation detection enhancement gels. *Electrophoresis* **17**, 1299–1301 (1996).
- Ganguly, A., Rock, M. J. & Prockop, D. Conformation sensitive gel electrophoresis for rapid detection of single-base differences in double-stranded PCR products and DNA fragments: evidence for solvent-induced bends in DNA heteroduplexes. *Proc. Natl Acad. Sci. USA* **90**, 10325–10329 (1993).
- Rice, N. R., MacKichan, M. L. & Israël, A. The precursor of NF-κB p50 has IκB-like functions. *Cell* **71**, 243–253 (1992).
- Weil, R., Laurent-Winter, C. & Israël, A. Regulation of IκBβ degradation—similarities and differences from IκBα. *J. Biol. Chem.* **272**, 9942–9949 (1997).
- Courtois, G., Whiteside, S. T., Sibley, C. H. & Israël, A. Characterization of a mutant cell line that does not activate NF-κB in response to multiple stimuli. *Mol. Cell. Biol.* **17**, 1441–1449 (1997).

Supplementary information is available on Nature's World-Wide Web site (<http://www.nature.com>) or as a paper copy from the London editorial office of Nature.

Acknowledgements

The IP Consortium thanks S. Emmerich, Director of the National Incontinentia Pigmenti Foundation, for financial and practical support, and for fostering a collaborative spirit throughout. We also thank the participating families for their cooperation, and their attending physicians for sharing information and facilitating enrolments: in particular V. Murday, S. Landy, J. Dean, M. C. Hors-Cayla, N. Dahl and M. Gonzales. This work has been supported by Action Research UK (S.J.K.); Association Française contre les Myodystrophies (A.M.); The Foundation Fighting Blindness; Research to Prevent Blindness, Inc.; (R.A.L.); the NIH (DLN); Telethon, Italy (M.D'U); Deutsche Forschungsgemeinschaft; the European Community (EC) Fifth Framework Programme (A.P.); Association pour la Recherche sur le Cancer, Ligue Nationale contre le Cancer and EC (A.I.) and by the National Incontinentia Pigmenti Foundation. R.A.L. is a Research to Prevent Blindness Senior Scientific Investigator. A.I. and G.C. thank C. Bessia for technical help.

Correspondence and requests for materials should be addressed to S.J.K. (e-mail: SJK12@mole.bio.cam.ac.uk).

* The International Incontinentia Pigmenta (IP) Consortium:

France: Asmae Smahi*†, G. Courtois‡, P. Vabres*, S. Yamaoka‡, S. Heuertz*, A. Munnich* & A. Israël‡
Germany: Nina S. Heiss†§, S. M. Klauß§, P. Kioschis§, S. Wiemann§ & A. Poustka§
Italy: Teresa Esposito†||, T. Bardarol||, F. Gianfrancesco||, A. Ciccodicola|| & M. D'Urso||
UK: Hayley Woffendin†¶, T. Jakins¶, D. Donnai#., H. Stewart# & S. J. Kenwright¶
USA: Swaroop Aradhya†☆☆, T. Yamagata**, M. Levy††, R. A. Lewis*** & D. L. Nelson***

* Department of Genetics, Unité de Recherches sur les Handicaps Génétiques de l'Enfant INSERMU-393, Hôpital Necker-Enfants Malades, 75015 Paris, France
 ‡ Unité de Biologie Moléculaire de l'Expression Génique URA 1773 CNRS, Institut Pasteur, 75724 Paris cedex 15, France
 § Deutsches Krebsforschungszentrum (DKFZ), Department of Molecular Genome Analysis, Im Neuenheimer Feld 280, 69120 Heidelberg, Germany
 || International Institute of Genetics and Biophysics, C.N.R. Via G. Marconi, 10, 80125 Naples, Italy
 ¶ Wellcome Trust Centre for Molecular Mechanisms of Disease and University of Cambridge Department of Medicine, Addenbrooke's Hospital, Hill Road, Cambridge CB2 2XY, UK
 # St Mary's Hospital, Whitworth Park, Manchester M13 0JH, UK
 Departments of **Molecular and Human Genetics, †† Dermatology and *** Ophthalmology, Baylor College of Medicine, Houston, Texas 77030, USA
 † These authors contributed equally to this work